Computers, Materials & Continua CMC, vol.64, no.1, pp.589-605, 2020

Generalized Array Architecture with Multiple Sub-Arrays and Hole-Repair Algorithm for DOA Estimation

Sheng Liu[1, *], Hailin Cao[2], Decheng Wu[2] and Xiyuan Chen[3]

Abstract: Arranging multiple identical sub-arrays in a special way can enhance degrees of freedom (DOFs) and obtain a hole-free difference co-array (DCA). In this paper, by adjusting the interval of adjacent sub-arrays, a kind of generalized array architecture with larger aperture is proposed. Although some holes may exist in the DCA of the proposed array, they are distributed uniformly. Utilizing the partial continuity of the DCA, an extended covariance matrix can be constructed. Singular value decomposition (SVD) is used to obtain an extended signal sub-space, by which the direction-of-arrival (DOA) estimation algorithm for quasi-stationary signals is given. In order to eliminating angle ambiguity caused by the holes of DCA, the estimation of signal parameters via rotational invariance techniques (ESPRIT) is used to construct a matrix that includes all angle information. Utilizing this matrix, a secondary extended signal sub-space can be obtained. This signal sub-space is corresponding to a hole-free DCA. Then, dealing with the further extended signal sub-space by multiple signal classification (MUSIC) algorithm, the unambiguous DOAs of all incident signals can be estimated. Some simulation results are shown to prove the improved performance of proposed generalized array architecture in DOA estimation and the effectiveness of corresponding hole-repair algorithm in eliminating angle ambiguity.

Keywords: Multiple sub-arrays, DOA estimation, difference co-array, hole-repair.

1 Introduction

Direction-of-arrival (DOA) estimation of spatial signals by using sensor array receives more and more attention because of its important application in the related fields such as wireless communication [Huang, Su, Wen et al. (2019); Su, Sheng, Leung et al. (2019)], radar system [Shi, Hu and Zhang (2018); Yang, Sun, Yuan et al. (2018); Liu, Wang, Li et al. (2018)] and electronic warfare. Aperture and DOFs of an array are two important factors to be considered, and they are related to the accuracy and angle

[1] School of Data Science, Tongren University, Tongren, 554300, China

[2] Laboratory of Aerocraft Tracking Telemetering Command and Communication, Chongqing University, Chongqing, 400044, China.

[3] Department of Mechanical Engineering, Stanford University, Stanford, 94305, USA.

[*] Corresponding Author: Sheng Liu. Email: liushengtrxy@126.com.

Received: 31 January 2020; Accepted: 29 February 2020.

resolution in DOA estimation.

Due to the limit of half-wavelength element spacing, the aperture and the DOFs of conventional uniform array are far less than the sparse array under the same number of sensors. For the sparse array, the element spacing of adjacent sensors can be different, and also can be larger than half-wavelength of received signal. Just for the different element spacing, many virtual sensors can be got by using the position difference of two sensors. The virtual array consisting of all virtual sensors is called as DCA. However, not all kinds of sparse array have the hole-free DCAs, i. e., the DCA can be seen as a uniform linear array (ULA) with consecutive virtual sensors. The existence of holes may affect the construction of extended covariance matrix, and cause direction ambiguity.

Minimum-redundancy array (MRA) [Moffet (1968)] is one of the classical sparse arrays with hole-free DCA. Under the same number of sensors, MRA can provide more consecutive virtual sensors than any other sparse arrays. Nevertheless, the irregularity of sensor positions makes us difficult to give the closed array configuration of MRA, particularly for larger number of sensors. Co-prime array [Vaidyanathan and Pal (2011); Pal and Vaidyanathan (2011)] consists of two uniform linear arrays, and two co-prime integers are used to determine the element intervals and the sensor number of the array. Co-prime array has regular array structure, and is effective in reducing the mutual couplings between two sensors. However, some co-prime arrays have not hole-free DCAs, and can cause angle ambiguity for DOA estimation. In literatures [Weng and Petar (2017); Zheng, Zhang and Gong (2017)], two effective methods have been presented to eliminate the angle ambiguity caused by the co-prime array. In addition, there are many other kinds of co-prime array constructions including generalized co-prime array [Qin, Zhang and Amin (2015)], co-prime L-shaped arrays [Ren, Wang and Chen (2016)], multi-period co-prime array [Gong, Zhang and Zheng (2018)], co-prime planar array [Zheng, Zhang and Xu (2018)] and co-prime MIMO radar [Shi, Hu and Zhang (2018)].

Nested array [Pal and Vaidyanathan (2010)] comprised by two uniform sub-arrays is another widely used sparse array with hole-free DCA. Many modified nested arrays were proposed to improve DOFs [Iizuka and Ichige (2017); Yang, Sun, Yuan et al. (2016); Liu, Zhang, Lu et al. (2017); Huang, Liao, Wang et al. (2017); Liu, Zhao, Wu et al. (2018)] and reducing mutual coupling [Liu, Zhang, Lu et al. (2017); Shi, Hu, Zhang et al. (2018)]. Particularly, nested arrays [Huang, Liao, Wang et al. (2017); Liu, Zhao, Wu et al. (2018)] can provider more DOFs than the other nested arrays. However, there are many irregular holes in the DCAs of the two nested arrays, which may lead to angle ambiguity in DOA estimation. Meanwhile, some other array constructions like nested L-shaped array [Liu, Yang, Li et al. (2017)], nested MIMO radar [Yang, Sun, Yuan et al. (2018); Liu, Wang, Li et al. (2018)] also were proposed based on the nested arrays [Pal and Vaidyanathan (2010); Yang, Sun, Yuan et al. (2016)].

In literature [Yang, Haimovich and Yuan (2018)], authors presented a unified sparse array construction which consists of multiple identical sub-arrays and has hole-free DCA. For this sparse array, all sub-arrays are arranged according to their DOFs and another given array geometry. Subsequently, a triple two-level nested array geometry [Liu, Liu, Zhao (2019)] was proposed, and it can propose more DOFs than the double two-level nested array in Yang et al. [Yang, Haimovich and Yuan (2018)].

In this paper, on basic of the array architecture Yang et al. [Yang, Haimovich and Yuan (2018)], we proposed a generalized array construction which consists of multiple sub-arrays with variable interval. Compared with the array Yang et al. [Yang, Haimovich and Yuan (2018)], the proposed generalized multiple-array construction has changeable and larger array aperture, and shows improved estimation accuracy in DOA. But the number of holes in DCA increases as the growth of the interval between adjacent sub-arrays. The appearance of holes will lead to direction ambiguity. In order to remedy the drawback of the generalized array architecture, a hole-repair algorithm also is proposed to eliminate angle ambiguity.

Notation: $[\bullet]^T$, $[\bullet]^H$, $E[\bullet]$ and $\otimes$ indicate transpose, conjugate transpose, statistical expectation and Kronecker product, respectively. $\mathbf{M}(i:j,:)$ represents a matrix consisting of the *i*th row to the *j*th row of matrix $\mathbf{M}$.

2 Data model

Suppose that K narrowband uncorrelated quasi-stationary signals are received by an L-element linear array. Denote $\theta_k, k=1,2,3,\cdots,K$ as the DOA of the kth source and d_w, $w=2,3,\cdots,W$ as the distance between the wth sensor and the reference sensor. The received vector $\boldsymbol{x}(t)=[x_1(t),x_2(t),\cdots,x_W(t)]^T \in C^{W\times 1}$ can be expressed as

$$\mathbf{x}(t)=\mathbf{A}\mathbf{s}(t)+\mathbf{n}(t) \tag{1}$$

where $\mathbf{A}=[\mathbf{a}(\theta_1),\mathbf{a}(\theta_2),\cdots,\mathbf{a}(\theta_K)]\in C^{W\times K}$ is array manifold matrix with $\mathbf{a}(\theta_k)=[1,e^{-i\frac{2\pi}{\lambda}d_2\sin(\theta_k)},\cdots e^{-i\frac{2\pi}{\lambda}d_W\sin(\theta_k)}]^T \in C^{W\times 1}$, $\mathbf{s}(t)=[s_1(t),s_2(t),\cdots,s_K(t)]^T \in C^{K\times 1}$ is signal vector and $\mathbf{n}(t)\in C^{W\times 1}$ represents Gaussian noise vector.

Assume that noise is uncorrelated from the signals and the covariance matrix of the fth frame can be written as Huang et al. [Huang, Liao, Wang et al. (2017); Liu, Zhao, Wu et al. (2018); Ma, Hsieh and Chi (2010)]

$$\begin{aligned}\mathbf{R}_f &= E\{\mathbf{x}(t)\mathbf{x}^H(t)\}\\ &= \mathbf{A}\mathbf{R}_{sq}\mathbf{A}^H+\mathbf{R}_n \in C^{L\times L}, t\in[(f-1)T, fT-1], f=1,2,\cdots,F\end{aligned} \tag{2}$$

where T is the number of snapshots in each frame, F is the number of frames, $\mathbf{R}_n=E\{\mathbf{n}(t)\mathbf{n}^H(t)\}$ is noise covariance matrix and $\mathbf{R}_{sf}=E\{\mathbf{s}_f(t)\mathbf{s}_f^H(t)\}$ is signal covariance matrix with the form as

$$\mathbf{R}_{sf}=\mathrm{diag}\{p_{f1}^2,p_{f2}^2,\cdots,p_{fK}^2\} \tag{3}$$

3 Generalized array architecture with multiple sub-arrays

Consider a ML-element generalized array construction which consists of M L-element fundamental linear arrays (FAs). M header sensors of the M FAs constitute a large-

spacing array (LA). We denote the $D(L)$ as the number of DOFs of the L-element FA and $D(M)$ be the number of DOFs of the M-element LA, respectively. Let the unit interval of the LA be $(D(L)+q)d$ with $q \geq 0$, $d = \frac{\lambda}{2}$, and the number of DOFs of the ML-element generalized array with multiple sub-arrays can be expressed as $D(L)D(M)$ [Yang, Haimovich and Yuan (2018)]. For convenience, when both the FA and LA are uniform linear arrays, we call the array construction as generalized double uniform array (GDUA). When both the FA and LA are nested arrays, we call the array construction as generalized double nested array (GDNA). We also call the two kinds of array construction as double uniform array (DUA) and double nested array (DNA) for q=0 .

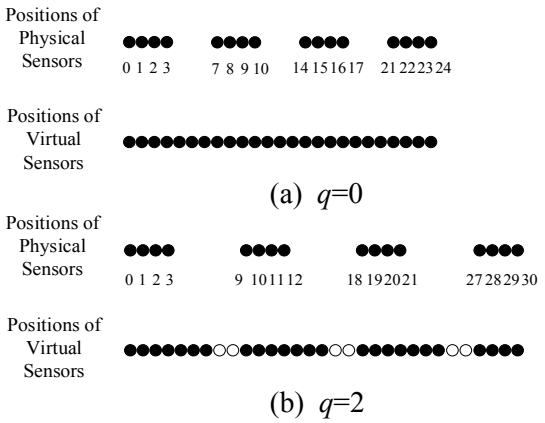

Figure 1: Construction of GDUA for q=0 and q=2, where hollow positions are "holes"

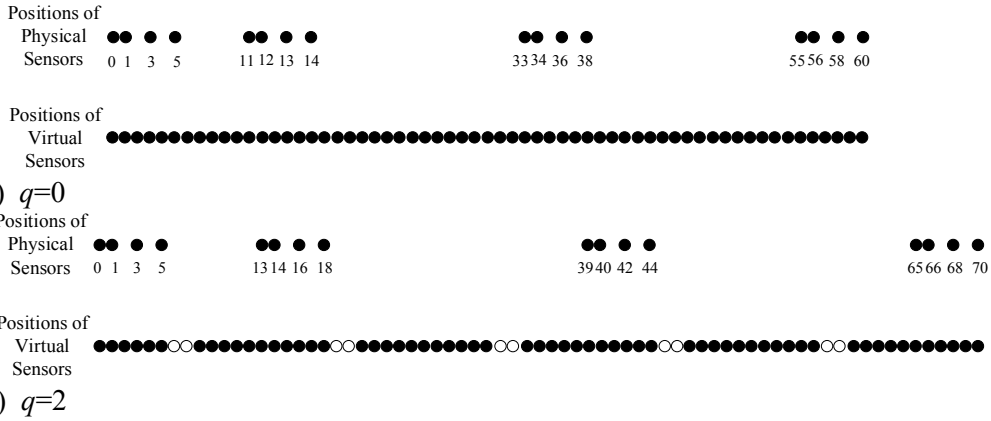

Figure 2: Construction of GDNA based on nested array [Pal and Vaidyanathan (2010)] for q=0 and q=2

We only take the GDUA and GDNA as example to introduce the proposed array construction. Fig. 1 shows two 16-element generalized GDUAs for q=0 and q=2. Fig. 2 and 3 show the 16-element generalized GDNAs based on nested array [Pal and Vaidyanathan (2010)] and improved nested array [Yang, Sun, Yuan et al. (2016)],

respectively. In the three groups of figures, the negative positions of virtual sensors are not listed. Adding the negative positions of virtual sensors, we can know that when $q > 0$, there are many holes in the DCAs. But we also can find that these holes are distributed uniformly. Hence, the virtual sensors can be divided into $D(M)$ groups, where each group consists of $D(L)$ successive virtual sensors, and q holes exist between two groups of successive virtual sensors.

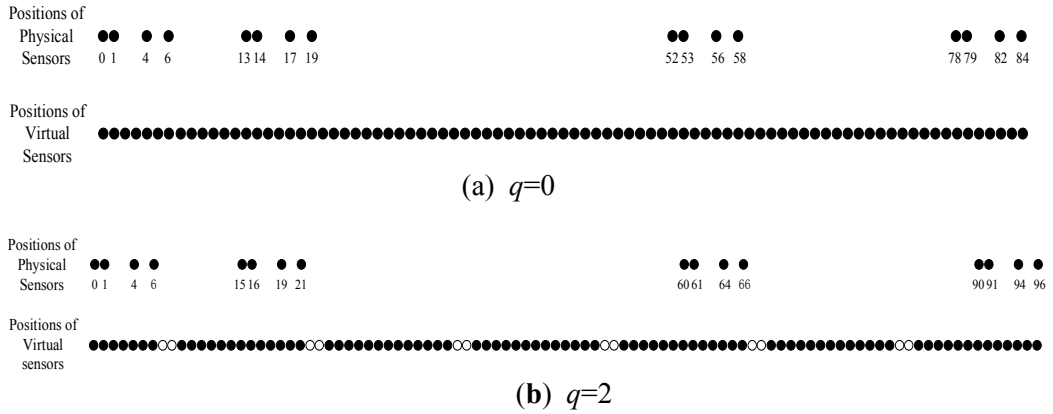

Figure 3: Construction of GDNA based on nested array [Yang, Sun, Yuan et al. (2016)] for q=0 and q=2

4 DOA estimation algorithm

As Pal et al. [Pal and Vaidyanathan (2011); Liu, Liu, Zhao (2019)], we can construct a covariance vector $\mathbf{c}_f \in C^{D(L)D(M)\times 1}$ in the fth frame. We should note that when q>0, $\mathbf{c}_f$ doesn't consist of the covariance with continuous sampling laps as co-prime [Pal and Vaidyanathan (2011)] and nested [Pal and Vaidyanathan (2010)]. Vector $\mathbf{c}_f$ can be expressed as

$$\mathbf{c}_f = \begin{bmatrix} \mathbf{c}_{-\frac{D(M)-1}{2},f} \\ \vdots \\ \mathbf{c}_{0,f} \\ \vdots \\ \mathbf{c}_{\frac{D(M)-1}{2},f} \end{bmatrix} + \delta_n \begin{bmatrix} 0 \\ \vdots \\ 1 \\ \vdots \\ 0 \end{bmatrix} \tag{4}$$

where $j = -\frac{D(M)-1}{2}, -\frac{D(M)-1}{2}+1, \cdots, 0, \cdots, \frac{D(M)-1}{2}-1, \frac{D(M)-1}{2}$, δ_n is the power of noise, and $\mathbf{c}_{j,f} \in C^{D(L)\times 1}$ can be expressed as

$$\mathbf{c}_{j,f}=\begin{bmatrix}\sum_{k=1}^{K}E\{\mathbf{s}_{kf}\mathbf{s}_{kf}^{H}\}e^{i\pi[(\frac{D(L)-1}{2})-j(D(L)+q)]\sin(\theta_k)}\\ \vdots\\ \sum_{k=1}^{K}E\{\mathbf{s}_{kf}\mathbf{s}_{kf}^{H}\}e^{i\pi[(\frac{D(L)-1}{2})-j(D(L)+q)-D(L)+1]\sin(\theta_k)}\end{bmatrix} \tag{5}$$

According to (5), we can know that though $\mathbf{c}_f$ may not consist of the covariance with continuous sampling laps, $\mathbf{c}_{j,f}$ consists of the covariance with continuous sampling laps. Substituting (5) into (4), we have

$$\mathbf{c}_f=\begin{bmatrix}\mathbf{A}_{-\frac{D(M)-1}{2}}\\ \vdots\\ \mathbf{A}_0\\ \vdots\\ \mathbf{A}_{\frac{D(M)-1}{2}}\end{bmatrix}\begin{bmatrix}E\{\mathbf{s}_{1f}\mathbf{s}_{1f}^{*}\}\\ \vdots\\ E\{\mathbf{s}_{Kf}\mathbf{s}_{Kf}^{*}\}\end{bmatrix}+\delta_n\begin{bmatrix}0\\ \vdots\\ 1\\ \vdots\\ 0\end{bmatrix} \tag{6}$$

where $\mathbf{A}_j\in C^{D(L)\times K}$ has the form as

$$\mathbf{A}_j=\begin{bmatrix}e^{i\pi[(\frac{D(L)-1}{2})-j(D(L)+q)]\sin(\theta_1)} & \cdots & e^{i\pi[(\frac{D(L)-1}{2})-j(D(L)+q)]\sin(\theta_K)}\\ \vdots & \cdots & \vdots\\ e^{i\pi[(\frac{D(L)-1}{2})-j(D(L)+q)-D(L)+1]\sin(\theta_1)} & \cdots & e^{i\pi[(\frac{D(L)-1}{2})-j(D(L)+q)-D(L)+1]\sin(\theta_K)}\end{bmatrix} \tag{7}$$

Using $\mathbf{c}_f$, we can construct a partitioned matrix as

$$\begin{aligned}\mathbf{C}&=\begin{bmatrix}\mathbf{c}_1 & \mathbf{c}_2 & \cdots & \mathbf{c}_F\end{bmatrix}\\ &=\begin{bmatrix}\mathbf{A}_{-\frac{D(M)-1}{2}}\\ \vdots\\ \mathbf{A}_0\\ \vdots\\ \mathbf{A}_{\frac{D(M)-1}{2}}\end{bmatrix}\begin{bmatrix}E\{\mathbf{s}_{11}\mathbf{s}_{11}^{*}\} & \cdots & E\{\mathbf{s}_{1F}\mathbf{s}_{1F}^{*}\}\\ \vdots & \cdots & \vdots\\ E\{\mathbf{s}_{K1}\mathbf{s}_{K1}^{*}\} & \cdots & E\{\mathbf{s}_{KF}\mathbf{s}_{KF}^{*}\}\end{bmatrix}+\delta_n\begin{bmatrix}0 & \cdots & 0\\ \vdots & \vdots & \vdots\\ 1 & \cdots & 1\\ \vdots & \vdots & \vdots\\ 0 & \cdots & 0\end{bmatrix}\end{aligned} \tag{8}$$

Denote two matrices $\tilde{\mathbf{A}}$ and Φ as

$$\tilde{\mathbf{A}} = \begin{bmatrix} \mathbf{A}_{-\frac{D(M)-1}{2}} \\ \vdots \\ \mathbf{A}_0 \\ \vdots \\ \mathbf{A}_{\frac{D(M)-1}{2}} \end{bmatrix} \tag{9}$$

$$\Phi = \begin{bmatrix} E\{\mathbf{s}_{11}\mathbf{s}_{11}^*\} & \cdots & E\{\mathbf{s}_{1F}\mathbf{s}_{1F}^*\} \\ \vdots & \cdots & \vdots \\ E\{\mathbf{s}_{K1}\mathbf{s}_{K1}^*\} & \cdots & E\{\mathbf{s}_{KF}\mathbf{s}_{KF}^*\} \end{bmatrix} \tag{10}$$

Then, formula (8) can be rewritten as

$$\mathbf{C} = \tilde{\mathbf{A}}\Phi + \begin{bmatrix} 0 \\ \vdots \\ \delta_n \\ \vdots \\ 0 \end{bmatrix} \mathbf{1}_F \tag{11}$$

where $\mathbf{1}_F \in C^{1\times F}$ is a matrix with all the elements being one.

As Ma et al. [Ma, Hsieh and Chi (2010)], we denote a matrix $\mathbf{P}_F^{\perp} = \mathbf{I}_F - (\mathbf{1}_F\mathbf{1}_F^T)/F$. Multiplying $\mathbf{C}$ with $\mathbf{P}_F^{\perp}$ yields

$$\mathbf{C}\mathbf{P}_F^{\perp} = \begin{bmatrix} \mathbf{A}_{-\frac{D(M)-1}{2}} \\ \vdots \\ \mathbf{A}_0 \\ \vdots \\ \mathbf{A}_{\frac{D(M)-1}{2}} \end{bmatrix} \Phi\mathbf{P}_F^{\perp} \tag{12}$$

Performing singular value decomposition (SVD) of $\mathbf{C}\mathbf{P}_F^{\perp}$, we can get

$$\mathbf{C}\mathbf{P}_F^{\perp} = \begin{bmatrix} \mathbf{U} & \mathbf{V} \end{bmatrix} \begin{bmatrix} \Sigma_s & 0 \\ 0 & 0 \end{bmatrix} \begin{bmatrix} \mathbf{U}^H \\ \mathbf{V}^H \end{bmatrix} \tag{13}$$

where $\mathbf{U}$ is the signal subspace consisting of the singular value vectors of K maximum singular values.

Denote the kth column of $\tilde{\mathbf{A}}$ as

$$\tilde{\mathbf{a}}(\theta_k)=\begin{bmatrix}\mathbf{a}_{-\frac{D(M)-1}{2}}(\theta_k)\\ \vdots\\ \mathbf{a}_0(\theta_k)\\ \vdots\\ \mathbf{a}_{\frac{D(M)-1}{2}}(\theta_k)\end{bmatrix} \tag{14}$$

where the concrete expression of $\mathbf{a}_j(\theta_k)$ is

$$\mathbf{a}_j(\theta_k)=\begin{bmatrix}e^{i\pi[(\frac{D(L)-1}{2})-j(D(L)+q)]\sin(\theta_k)}\\ \vdots\\ e^{i\pi[(\frac{D(L)-1}{2})-j(D(L)+q)-D(L)+1]\sin(\theta_k)}\end{bmatrix} \tag{15}$$

Denote $\mathbf{U}_o$ as the Smith normalization vector of $\mathbf{U}_o$. As MUSIC algorithm [Schmidt (1986)], maximizing the function

$$g(\theta)=\frac{1}{\tilde{\mathbf{a}}^H(\theta)(\mathbf{I}-\mathbf{U}_o\mathbf{U}_o^H))\tilde{\mathbf{a}}(\theta)} \tag{16}$$

we can get the DOA estimation of all signals.

It is all known that holes of DCA can lead to angle ambiguity when the number of signals is larger. For remedying the drawback of the proposed generalized array construction, a hole-repair algorithm will be proposed on the basis of the conventional MUSIC algorithm in the following text.

5 DOA estimation with hole-repair

Angle ambiguity is due to the un-continuity of DCA, namely the existence of hole. In fact, the existence of hole also can be seen as the element absence of manifold matrix $\tilde{\mathbf{A}}$ which leads to the element absence of signal subspace $\mathbf{U}$. If we can reconstruct a new subspace which corresponds to a new manifold matrix without missing elements, angle ambiguity can be eliminated.

Firstly, we denote three matrices $\mathbf{A}_{j,1}\in C^{(D(L)-1)\times K}$, $\mathbf{A}_{j,2}\in C^{(D(L)-1)\times K}$ and $\mathbf{A}_{j,3}\in C^{q\times K}$ as

$$\begin{cases}\mathbf{A}_{j,1}=\mathbf{A}_j(1:D(L)-1,:)\\ \mathbf{A}_{j,2}=\mathbf{A}_j(2:D(L),:)\\ \mathbf{A}_{j,3}=\mathbf{A}_j(D(L)-q+1:D(L),:)\end{cases} \tag{17}$$

Then, we construct three block matrices $\mathbf{A}_1\in C^{D(M)(D(L)-1)\times K}$, $\mathbf{A}_2\in C^{D(M)(D(L)-1)\times K}$ and $\mathbf{A}_3\in C^{q(D(M)-1)\times K}$ as

$$\begin{cases} \mathbf{A}_1 = \left[\mathbf{A}^T_{-\frac{D(M)-1}{2},1} \quad \cdots \quad \mathbf{A}^T_{0,1} \quad \cdots \quad \mathbf{A}^T_{\frac{D(M)-1}{2},1} \right]^T \\ \mathbf{A}_2 = \left[\mathbf{A}^T_{-\frac{D(M)-1}{2},2} \quad \cdots \quad \mathbf{A}^T_{0,2} \quad \cdots \quad \mathbf{A}^T_{\frac{D(M)-1}{2},2} \right]^T \\ \mathbf{A}_3 = \left[\mathbf{A}^T_{-\frac{D(M)-1}{2},3} \quad \cdots \quad \mathbf{A}^T_{0,3} \quad \cdots \quad \mathbf{A}^T_{\frac{D(M)-3}{2},3} \right]^T \end{cases} \tag{18}$$

According to Eqs. (17) and (18), we have

$$\mathbf{A}_2 = \mathbf{A}_1 \Psi \tag{19}$$

where $\Psi = diag\{e^{-i\pi\sin(\theta_1)}, e^{-i\pi\sin(\theta_2)}, \cdots, e^{-i\pi\sin(\theta_K)}\}$.

According to the construction of $\tilde{\mathbf{A}}$, we rewrite the signal subspace $\mathbf{U}$ as

$$\mathbf{U} = \begin{bmatrix} \mathbf{U}_{-\frac{D(M)-1}{2}} \\ \vdots \\ \mathbf{U}_0 \\ \vdots \\ \mathbf{U}_{\frac{D(M)-1}{2}} \end{bmatrix} \tag{20}$$

As (17-19), we denote three matrices $\mathbf{U}_{j1} \in C^{(D(L)-1)\times K}$, $\mathbf{U}_{j2} \in C^{(D(L)-1)\times K}$ and $\mathbf{U}_{j3} \in C^{q\times K}$ as

$$\begin{cases} \mathbf{U}_{j1} = \mathbf{U}_j(1:D(L)-1,:) \\ \mathbf{U}_{j2} = \mathbf{U}_j(2:D(L),:) \\ \mathbf{U}_{j3} = \mathbf{U}_j(D(L)-q+1:D(L),:) \end{cases} \tag{21}$$

Then, we construct three block matrices $\mathbf{U}_1 \in C^{D(M)(D(L)-1)\times K}$, $\mathbf{U}_2 \in C^{D(M)(D(L)-1)\times K}$ and $\mathbf{U}_3 \in C^{q(D(M)-1)\times K}$ as

$$\begin{cases} \mathbf{U}_1 = \left[\mathbf{U}^T_{-\frac{D(M)-1}{2},1} \quad \cdots \quad \mathbf{U}^T_{0,1} \quad \cdots \quad \mathbf{U}^T_{\frac{D(M)-1}{2},1} \right]^T \\ \mathbf{U}_2 = \left[\mathbf{U}^T_{-\frac{D(M)-1}{2},2} \quad \cdots \quad \mathbf{U}^T_{0,2} \quad \cdots \quad \mathbf{U}^T_{\frac{D(M)-1}{2},2} \right]^T \\ \mathbf{U}_3 = \left[\mathbf{U}^T_{-\frac{D(M)-1}{2},3} \quad \cdots \quad \mathbf{U}^T_{0,3} \quad \cdots \quad \mathbf{U}^T_{\frac{D(M)-3}{2},3} \right]^T \end{cases} \tag{22}$$

According to ESPRIT algorithm [Richard and Kailath (1989)], we can know that there is an invertible matrix $\mathbf{T}$ meeting

$$\begin{cases} \mathbf{U}_1\mathbf{T}=\mathbf{A}_1 \\ \mathbf{U}_2\mathbf{T}=\mathbf{A}_2 \\ \mathbf{U}_3\mathbf{T}=\mathbf{A}_3 \end{cases} \tag{23}$$

According to (23), we have

$$\mathbf{U}_1^{+}\mathbf{U}_2=\mathbf{T}\Psi\mathbf{T}^{-1} \tag{24}$$

From (24), it's easy to drive

$$(\mathbf{U}_1^{+}\mathbf{U}_2)^q=\mathbf{T}\Psi^q\mathbf{T}^{-1} \tag{25}$$

Multiplying $(\mathbf{U}_1^{+}\mathbf{U}_2)^q$ by $\mathbf{U}_3$ and $\mathbf{T}$, we have

$$\mathbf{U}_3(\mathbf{U}_1^{+}\mathbf{U}_2)^q\mathbf{T}=\mathbf{U}_3\mathbf{T}\Psi^q=\mathbf{A}_3\Psi^q \tag{26}$$

Suppose that $\mathbf{0}_{s\times r}$ represents a $s\times r$ null matrix and $\mathbf{I}_s$ represents an s-order unit matrix. Then we construct two matrices as

$$\mathbf{G}_1=\begin{bmatrix} \mathbf{I}_{D(M)-1}\otimes\begin{bmatrix}\mathbf{I}_{D(L)}\\ \mathbf{0}_{q\times D(L)}\end{bmatrix} & \mathbf{0}_{[(D(M)-1)(D(L)+q)]\times D(L)} \\ \mathbf{0}_{D(L)\times[D(L)(D(M)-1)]} & \mathbf{I}_{D(L)} \end{bmatrix} \tag{27}$$

$$\mathbf{G}_2=\begin{bmatrix} \mathbf{I}_{D(M)-1}\otimes\begin{bmatrix}\mathbf{0}_{D(L)\times q}\\ \mathbf{I}_{q\times q}\end{bmatrix} \\ \mathbf{0}_{D(L)\times[(D(M)-1)q]} \end{bmatrix} \tag{28}$$

Denoting a new matrix as $\bar{\mathbf{A}}=\mathbf{G}_1\otimes\tilde{\mathbf{A}}+\mathbf{G}_2\otimes\mathbf{A}_3\Psi^q\in C^{[D(L)D(M)+q(D(M)-1)]\times K}$ and rewriting the $\bar{\mathbf{A}}$ in the form $\bar{\mathbf{A}}=[\bar{\mathbf{a}}(\theta_1),\bar{\mathbf{a}}(\theta_2),\cdots,\bar{\mathbf{a}}(\theta_K)]$, we can get that $\bar{\mathbf{a}}(\theta_k)=[e^{i\pi\frac{[D(L)D(M)+q(D(M)-1)-1]}{2}\sin(\theta_k)},\cdots,e^{i\pi\sin(\theta_k)},1,e^{-i\pi\sin(\theta_k)},\cdots,e^{-i\pi\frac{[D(L)D(M)+q(D(M)-1)-1]}{2}\sin(\theta_k)}]^T$ $\in C^{[D(L)D(M)+q(D(M)-1)]\times 1}$

According to (28), we have

$$\mathbf{U}_{new}=\mathbf{G}_1\otimes\mathbf{U}+\mathbf{G}_2\otimes\mathbf{U}_3(\mathbf{U}_1^{+}\mathbf{U}_2)^q=\bar{\mathbf{A}}\mathbf{T} \tag{29}$$

Denote $\mathbf{U}_{newo}$ as the Smith normalization vector of $\mathbf{U}_{new}$. Maximizing the new function

$$g_{new}(\theta)=\frac{1}{\bar{\mathbf{a}}^H(\theta)(\mathbf{I}-\mathbf{U}_{newo}\mathbf{U}_{newo}{}^H)\bar{\mathbf{a}}(\theta)} \tag{30}$$

we can get the DOA estimation without angle ambiguity. Obviously, matrix $\bar{\mathbf{A}}$ can be seen as a manifold matrix of a hole-free DCA. Hence, we call the above-mentioned process as hole-repair algorithm.

6 Simulation

In this section, we present several groups of simulation experiments to test the performance of the proposed general generalized array construction in DOA estimation. All simulation experiments are performed by Matlab2017b on the computer with Windows 2010 system, 8 GB RAM and 1.8 GHz CPU. We only take the 16-element GDUA and GDNA as example. Suppose that the search range is from -90° to 90° and the search interval is 0.1° in each DOA estimation process. The formula for calculating the root mean square error (RMSE) is given as

$$\mathrm{RMSE}=\sqrt{\frac{1}{KJ}\sum_{j=1}^{J}\sum_{k=1}^{K}(\hat{\theta}_{kj}-\theta_k)^2} \tag{31}$$

where $\hat{\theta}_{kj}$ is the estimation of θ_k in the jth experiment, and j=500.

6.1 Comparison of music spectra

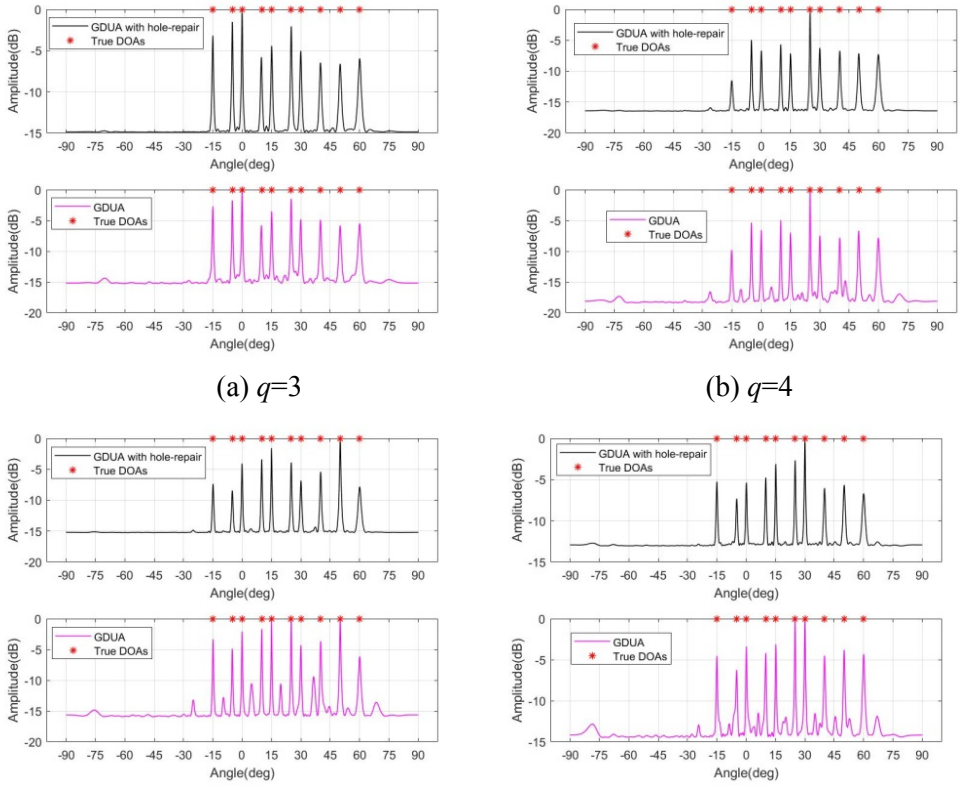

(a) q=3 (b) q=4

(c) q=5 (d) q=6

Figure 4: Comparison of MUSIC spectra for GDUA and GDUA with hole-repair

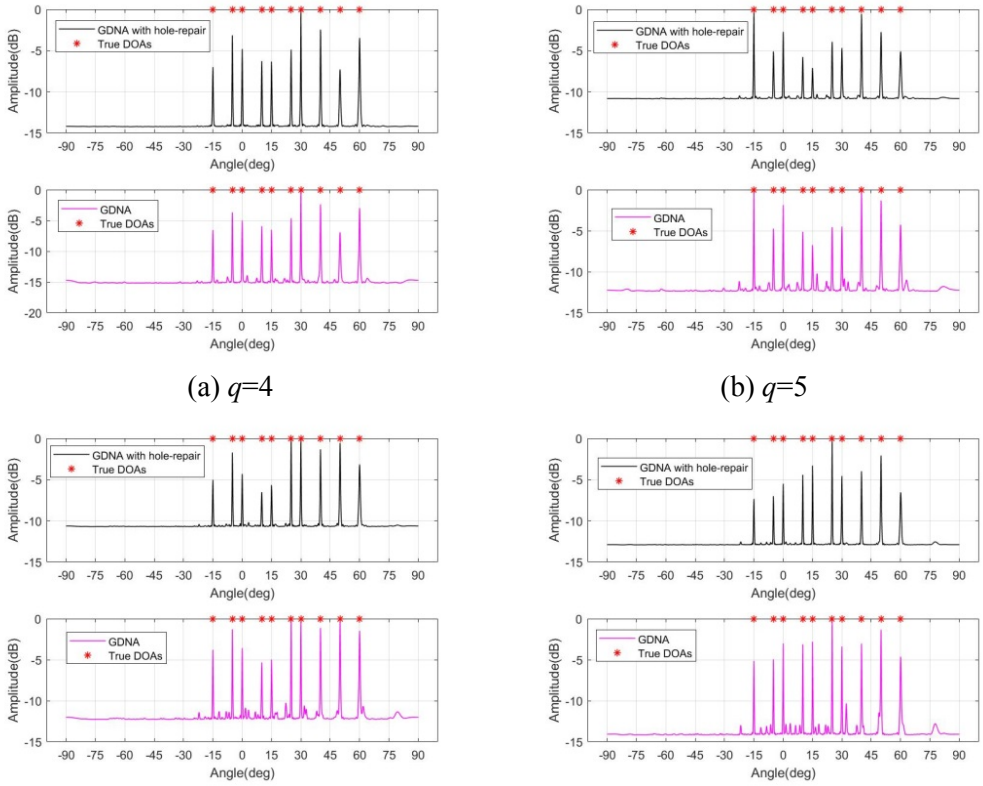

(a) q=4 (b) q=5

(c) q=6 (d) q=7

Figure 5: Comparison of MUSIC spectra for GDNA and GDNA with hole-repair

In this subsection, we test the validity of the hole-repair algorithm in eliminating angle ambiguity. Suppose that the DOAs of 10 signals are -15°, -5°, 0°, 10°,15°, 25°, 30°, 40°, 50°, 60°, respectively. The number of snapshots in one frame is 200, the number of frame is 40 and SNR is fixed at 5 dB. The nested array [Pal and Vaidyanathan (2010)] is used as FA and LA to construct the GDNA. Fig. 4 shows the comparison of MUSIC spectra for GDUA and GDUA with hole-repair algorithm. Fig. 5 shows the comparison of MUSIC spectra for GDNA and GDNA with hole-repair algorithm. Observing the difference in every comparative figure, for the GDUA and GDNA, we can find that both the number and amplitude of false spectrum peaks increase with q. But, we also can see that there is almost no obvious false spectrum peaks after the hole-repair algorithm is used. The results shown in these figures can prove the effectiveness of proposed hole-repair algorithm in eliminating angle ambiguity.

6.2 Comparison of RMSE

Firstly, we compare the RMSE of DOA estimation by DUA and GDUA. Suppose that the direct angles of 8 signals are -30°, -20°, -10° 0°, 10°, 20°, 30°, 40°, respectively. Fig. 6 depicts the comparison of RMSE versus the SNR for different q under the condition that

T=400 and F=60. Fig.7 depicts the RMSE versus the snapshots for different q under the condition that F=60 and SRN=0 dB. Fig. 8 depicts the RMSE versus the number of frames for different q under the condition that T=400 and SNR=0 dB. DUA [Yang, Haimovich and Yuan (2018)] also can be seen as the case that q=0. Observing the comparative results shown in Fig. 6, Fig. 7 and Fig. 8, we can find that the RMSE of DOA estimation based on GDUA is lower than the DUA.

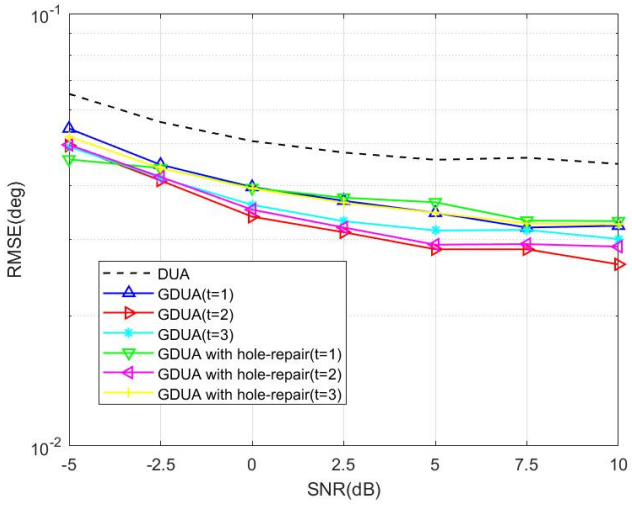

Figure 6: RMSE against SNR for DUA and GDUA

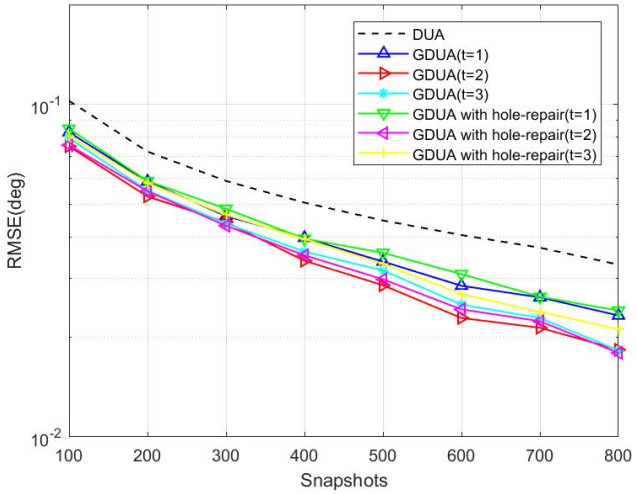

Figure 7: RMSE against snapshots for DUA and GDUA

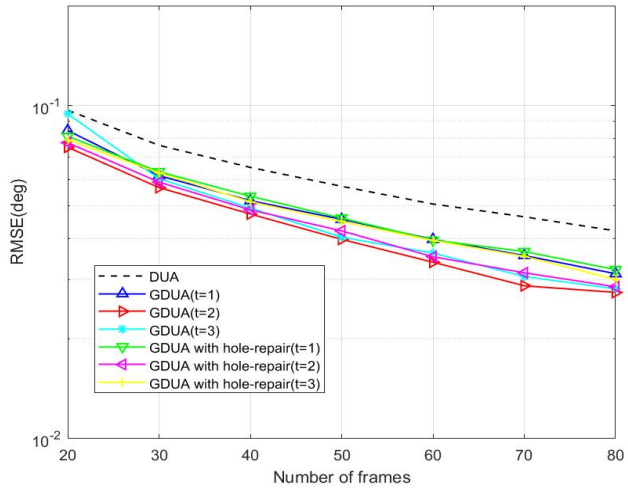

Figure 8: RMSE against the number of frames for DUA and GDUA

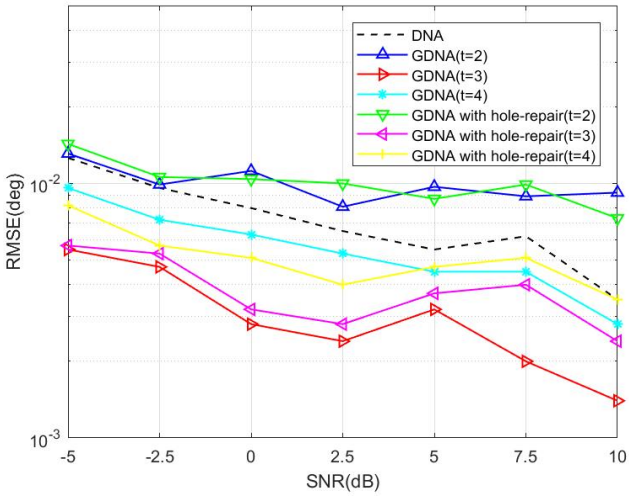

Figure 9: RMSE against SNR for DNA and GDNA

Then, we compare the RMSE of DOA estimation by DNA and GDNA. Suppose that the direct angles of 10 signals are -40°, -30°, -20°, -10°, 0°, 10°, 20°, 30°, 40°, 50°, respectively. Here the GDNA is based on the nested array [Yang, Sun, Yuan et al. (2016)]. Fig. 9 depicts the comparison of RMSE *vs.* the SNR for different q under the condition that T=200 and F=40. Fig. 10 depicts the RMSE *vs.* the number of frames for different q under the condition that with T=200 and SNR=0 dB. Observe the comparative results shown in Figs. 9 and 10, we can find that the RMSE of DOA estimation based on GDUA is lower than the DUA as q>2. Because 16-element DNA already has larger aperture, smaller q only has little effect in extending array aperture. From Figs. 1 and 3, we find that the DOFs of 16-element DUA are far smaller than the DNA. In this case,

smaller q also has effect in extending aperture and improving the DOA estimation precision.

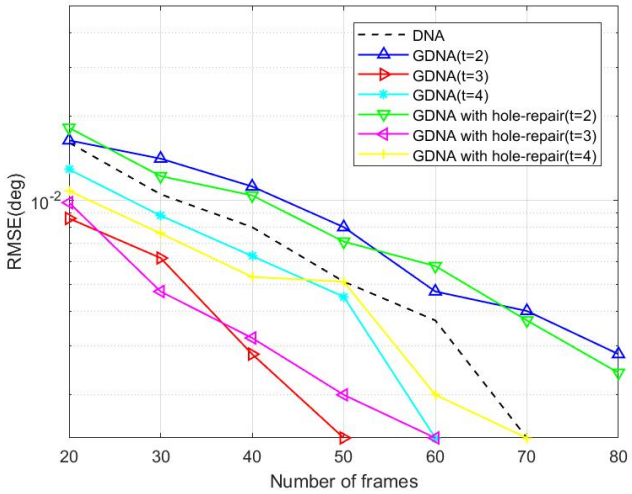

Figure 10: RMSE against the number of frames for DNA and GDNA

7 Conclusion

In this paper, the generalized array architecture with multiple sub-arrays is presented. By changing the interval of adjacent sub-arrays, we can get many kinds of generalized array architecture with larger aperture than the original array. Meanwhile, a hole-repair algorithm is also proposed to remove the false spectrum peaks caused by the holes of corresponding DCA. In simulation experiments, GDUA based on uniform liner array and GDNA based on nested array are taken as example to test the performance of generalized array architecture in DOA estimation. Simulation results also prove that the hole-repair algorithm is effective in removing false spectrum peaks and eliminating angle ambiguity.

Funding Statement: This work was supported by supported by the National Natural Science Foundation of China (51877015, U1831117), the Cooperation Agreement Project by the Department of Science and Technology of Guizhou Province of China (LH [2017] 7320, LH [2017] 7321), the Foundation of Top-notch Talents by Education Department of Guizhou Province of China (KY [2018] 075), the nature and science fund from the Education Department of Guizhou province the Innovation Group Major Research Program Funded by Guizhou Provincial Education Department (KY [2016] 051) and PhD Research Startup Foundation of Tongren University (trxyDH1710).

Conflicts of Interest: The authors declare that they have no conflicts of interest to report regarding the present study.

References

Gong, P.; Zhang, X.; Zheng, W. (2018): Unfolded coprime L-shaped arrays for two-dimensional direction of arrival estimation. *International Journal of Electronics*, vol. 105, no. 9, pp. 1501-1519.

Huang, H.; Liao, B.; Wang, X.; Guo, X.; Huang, J. (2017): A new nested array configuration with increased degrees of freedom. *IEEE Access*, vol. 6, pp. 1490-1497.

Huang, Z.; Su, J.; Wen G. J.; Zheng, W.; Chu, C. et al. (2019): A physical layer algorithm for estimation of number of tags in UHF RFID anti-collision design, *Computers, Materials & Continua*, vol. 61, no. 1, pp. 399-408.

Iizuka, Y.; Ichige, K. (2017): Extension of nested array for large aperture and high degree of freedom. *IEICE Communications Express*, vol. 6, no. 6, pp. 381-386.

Liu, J.; Zhang, Y.; Lu, Y.; Ren, S.; Cao, S. (2017): Augmented nested arrays with enhanced DOF and reduced mutual coupling. *IEEE Transactions on Signal Processing*, vol. 65, no. 21, pp. 5549-5563.

Liu, Q.; Wang, B.; Li, X.; Tian, J.; Cheng, T. et al. (2018): An optimizing nested MIMO array with hole-free difference coarray. *MATEC Web of Conferences*, pp. 01055.

Liu, S.; Liu, Q.; Zhao, J.; Yuan, Z. (2019): Triple two-level nested array with improved degrees of freedom. *Progress in Electromagnetics Research B*, vol. 84, pp. 135-151.

Liu, S.; Yang, L.; Li, D.; Cao, H. (2017): Subspace extension algorithm for 2D DOA estimation with L-shaped sparse array. *Multidimensional Systems and Signal Processing*, vol. 28, no. 1, pp. 315-327.

Liu, S.; Zhao, J.; Wu, D.; Cao, H. (2018): Grade nested array with increased degrees of freedom for quasi-stationary signals. *Progress in Electromagnetics Research Letters*, vol. 80, pp. 75-82.

Ma, W. K.; Hsieh, T. H.; Chi, C. Y. (2010): DOA estimation of quasi-stationary signals with less sensors than sources and unknown spatial noise covariance a Khatri-Rao subspace approach. *IEEE Transactions on Signal Processing*, vol. 58, no. 4, pp. 2168-2180.

Moffet, A. (1968): Minimum-redundancy linear arrays. *IEEE Transactions on Antennas and Propagation*, vol. 16, no. 2, pp. 172-175.

Pal, P.; Vaidyanathan, P. P. (2011): Co-prime sampling and the MUSIC algorithm. *Proceedings of Digital Signal Processing Work Shop and IEEE Signal Processing Education Work Shop*, pp. 289-294.

Pal, P.; Vaidyanathan, P. P. (2010): Nested arrays: a novel approach to array processing with enhanced degrees of freedom. *IEEE Transactions on Signal Processing*, vol. 58, no. 8, pp. 4167-4181.

Qin, S.; Zhang, Y. D.; Amin, M. G. (2015): Generalized co-prime array configurations for direction-of-arrival estimation. *IEEE Transactions on Signal Processing*, vol. 63, no. 6, pp. 1377-1390.

Ren, S. W.; Wang, W. J.; Chen, Z. H. (2016): DOA estimation exploiting unified coprime array with multi-period subarrays. *Proceedings of CIE International Conference on Radar*, pp. 1-4.

Richard, R.; Kailath, T. (1989): ESPRIT-estimation of signal parameters via rotational invariance techniques. *IEEE Transactions on Acoustics Speech and Signal Processing*, vol. 37, no. 7, pp. 984-995.

Schmidt, R. O. (1986): Multiple emitter location and signal parameter estimation. *IEEE*

Transactions on Antennas and Propagation, vol. 34, no. 3, pp. 276-280.
Shi, J., Hu, G.; Zhang, X. (2018): Generalized co-prime MIMO radar for DOA estimation with enhanced degrees of freedom. *IEEE Sensors Journal*, vol. 18, no. 3, pp. 1203-1212.
Shi, J.; Hu, G.; Zhang, X.; Zhou, H. (2018): Generalized nested array: optimization for degrees of freedom and mutual coupling. *IEEE Communication Letters*, vol. 22, no. 6, pp. 1208-1211.
Su, J.; Sheng, Z.; Leung, V. C. M.; Chen, Y. (2019): Energy efficient tag identification algorithms for RFID: survey, motivation and new design. *IEEE Wireless Communications*, vol. 26, no. 3, pp. 118-124.
Vaidyanathan, P. P.; Pal, P. (2011): Sparse sensing with co-prime samplers and arrays. *IEEE Transactions on Signal Processing*, vol. 59, no. 2, pp. 573-586.
Weng, Z. Y.; Petar, M. D. (2014): A search-free DOA estimation algorithm for co-prime arrays. *Digital Signal Processing*, vol. 24, pp. 27-33.
Yang, M.; Sun, L.; Yuan, X.; Chen, B. (2016): Improved nested array with hole-free DCA and more degrees of freedom. *Electronics Letters*, vol. 52, no. 25, pp. 2068-2070.
Yang, M.; Sun, L.; Yuan, X.; Chen, B. (2018): A new nested MIMO array with increased degrees of freedom and hole-free difference co-array. *IEEE Signal Processing Letters*, vol. 25, no. 1, pp. 40-44.
Yang, M.; Haimovich, A. M.; Yuan, X. (2018): A unified array geometry composed of multiple identical sub-arrays with hole-free difference co-arrays for underdetermined DOA estimation. *IEEE Access*, vol. 6, pp. 14238-14254.
Zheng, W.; Zhang, X.; Gong, P. (2017): DOA estimation for co-prime linear arrays: an ambiguity-free method involving full DOFs. *IEEE Communication Letters*, vol. 3, no. 22, pp. 562-565.
Zheng, W.; Zhang, X.; Xu, L. (2018): Unfolded co-prime planar array for 2D direction of arrival estimation: an aperture-augmented perspective. *IEEE Access*, vol. 6, pp. 22744-22753.